



The lapachol derivatives from *Tabebuia aurea*: distribution and cytotoxic evaluation against human cancer cells

Rahmat Kurniawan^{1*}, Arif Ashari¹, Muhammad Yogi Saputra¹, Indarto¹, Peni Ahmadi², Tati Suhartati³

¹Chemistry Department, Institute of Technology Sumatera, South Sumatera, Indonesia.

²Research Center for Vaccine and Drugs, National Research and Innovation Agency, Jakarta Pusat, Indonesia.

³Chemistry, Department of Sciences, Lampung University, Lampung, Indonesia.

ARTICLE HISTORY

Received on: 23/11/2025

Accepted on: 06/03/2026

Available Online: 15/04/2026

Key words:

Tabebuia aurea, lapachol derivatives, cytotoxic activity, human cancer cells.

ABSTRACT

The *Tabebuia aurea* (Bignoniaceae) is recognized as a plant with significant ethnomedicinal potential. Species within the *Tabebuia* sp. have long been utilized in traditional medicine for the treatment of various conditions, including infectious diseases, inflammatory disorders, and metabolic syndromes. This study reports the isolation, screening of naphthoquinone content and cytotoxic evaluation of three lapachol derivatives, lapachol (**1**), α -lapachone (**2**), and β -lapachone (**3**), from the bark of *T. aurea*. The bark extracts yielded the highest concentrations of these naphthoquinones, with acetone providing the greatest retrieval by 36.62 ± 2.44 ppm. Among the isolates, β -lapachone demonstrated the strongest cytotoxic activity against HeLa, MCF-7, and A549 cell lines with IC_{50} values of 6.24 ± 0.52 , 2.85 ± 0.26 , and 5.61 ± 0.88 μ M, respectively. Solvent polarity and tissue type markedly influenced metabolite distribution, identifying bark-acetone as the optimal source of bioactive naphthoquinones. The results provide insight into the therapeutic potential of *T. aurea* and contribute to the upward evidence supporting its dual role in biodiversity restoration and herbal medicine development.

1. INTRODUCTION

The genus *Tabebuia* (family Bignoniaceae) comprises approximately 100 species of flowering trees predominantly distributed across tropical and subtropical regions. The genus name, first introduced in the early 19th century, originates from the term “tacyba bebuya”, meaning “ant wood”, referring to ants inhabiting the hollow branches of some species [1]. These species have been the focus of numerous phytochemical and pharmacological studies due to their rich diversity of bioactive secondary metabolites [2–4]. Traditionally, various *Tabebuia* species have been employed in traditional medicine to manage ailments including diabetes, ulcers, syphilis, and infectious diseases [5]. Indigenous communities have

traditionally employed these extracts as natural remedies for the management of snake envenomation [6]. Extracts from the genus have demonstrated a wide range of biological activities, notably anti-inflammatory, cytotoxic, antimicrobial, and immunomodulatory effects [7,8].

Phytochemical investigations have revealed that certain secondary metabolites present in *Tabebuia*, such as lapachol, possess noteworthy bioactivities [5]. Lapachol has been extensively examined for its potential application as an adjunct agent in anticancer treatment. Collectively, these results emphasize the genus as an important reservoir of pharmacologically relevant bioactive compounds [9]. The compound lapachol (**1**), a naturally occurring naphthoquinone first identified in the heartwood of red lapacho (*Tabebuia* sp), initially attracted considerable scientific interest due to its reported anticancer activity [10]. However, subsequent phase I clinical trials revealed toxicity and a lack of therapeutic efficacy, leading to its discontinuation by the National Cancer Institute [3,11]. Despite the promising biological activity observed in early clinical trials, the further development of lapachol was

*Corresponding Author

Rahmat Kurniawan, Chemistry Department, Institute of Technology Sumatera, South Sumatera, Indonesia. E-mail: rahmat.kurniawan@ki.itera.ac.id

constrained by toxicity and unfavorable pharmacokinetic properties [12,13]. These limitations interested the exploration of structurally related isomers, particularly β - and α -lapachones, which display distinct redox characteristics and improved bioactivity profiles [14,15]. Notably, these derivatives have been reported to preserve or enhance the anticancer potential of lapachol while reducing the adverse effects identified in previous clinical investigations [10,16].

The *T. aurea* is a flowering tree species utilized in the reforestation and landscape restoration efforts of the Institut Teknologi Sumatera (ITERA) Botanical Garden in South Lampung, Indonesia. This species is valued for its strong adaptability to local environmental conditions and its visually appealing, bright yellow blossoms. Traditionally, the stem tea of *T. aurea* has been used in topical herbal remedies for treating warts and calluses [17]. The present study investigates the presence of lapachol derivative compounds in *T. aurea* through phytochemical screening and structural elucidation, and evaluates their cytotoxic potential against breast, lung, and cervical cancer cell lines using the MTT assay. This research aims to provide scientific support for the dual role of *T. aurea* in green space development and as a potential source of herbal medicine.

2. MATERIALS AND METHODS

2.1. Plant samples

Specimens of *T. aurea* were collected in June 2024 from the ITERA Botanical Garden, located in South Lampung, Sumatra, Indonesia (coordinates: 5°22'12.1"S, 105°18'47.9"E). Taxonomic identification was confirmed by the Bogor Herbarium, and a sample specimen has been archived at the ITERA Botanical Garden under accession number FA.12625.

2.2. General procedures

The general research procedures were conducted following the method developed by Kurniawan *et al.* [18] and were carried out at the Natural Products Laboratory, ITERA. Plant materials from *T. aurea* were subjected to extraction using methanol by maceration. The resulting crude extract was fractionated and purified through column chromatography, employing silica gel 7,734 (particle size: 0.063–0.2 mm) and Sephadex (Merck) as stationary phases. The progress of separation was monitored by thin-layer chromatography (TLC) on silica gel PF254 plates, visualized under UV light at 254 and 366 nm. The structures of the lapachol derivatives were determined by Bruker NMR spectroscopy using ^1H and ^{13}C NMR (500 and 125 MHz, respectively), with deuterated chloroform (CDCl_3) the solvent and tetramethylsilane as the internal standard. Functional group analysis was performed with a PerkinElmer Fourier transform infrared spectroscopy spectrometer. Mass spectra were obtained using an HP 5973 instrument coupled with a JEOL JMS Ax-500 mass spectrometer. Quantitative analysis of lapachol derivatives was conducted by a Genesys 150 UV-Visible spectrophotometer (Thermo Scientific).

2.3. Extraction and Isolation

Dried stem bark powder of *T. aurea* (2,000 g) was subjected to maceration by methanol (1 L) four times

at 30°C–34°C under reduced pressure, resulting in 84.4 g of crude methanolic extract. The stem bark was selected because it is a primary site for the accumulation of bioactive secondary metabolites and is also the plant part traditionally used for medicinal purposes [6,7]. The total extraction time was approximately 96 hours. Solvent removal was performed using rotary evaporation at 45°C under vacuum. The crude extract was partitioned sequentially with solvents of increasing polarity to yield hexane (16.5 g), ethyl acetate (28.7 g), and acetone (10.6 g) fractions. Fractionation was performed based on chromatographic performance rather than bioactivity screening. A 20 g portion of the ethyl acetate fraction was subjected to silica gel column chromatography using a gradient elution of hexane-ethyl acetate-methanol (0%–100%), affording 48 subfractions. Subfractions 12–19 (542 mg) were combined according to TLC profiles and further purified by size-exclusion chromatography on a Sephadex LH-20 column (methanol–chloroform, 1:1, v/v), yielding 32 fractions. Fractions 5–7 were subjected to three successive Sephadex LH-20 separations (2.5 × 50 cm, methanol, 0.5 ml/minute), affording compounds (1) (18.3 mg) and (2) (16.7 mg). Independently, subfractions 22–27 (213.1 mg) were chromatographed over silica gel to produce 12 fractions, from which fractions 3–7 yielded compound (3) (13.9 mg). In addition, fraction 15 was recrystallized from methanol to afford an additional 5.3 mg of compound (1).

2.4. The lapachol-derived determination content

The content screening method was adapted from Kurniawan *et al.* [18]. Quantification of lapachol derivatives compounds was performed by UV–visible spectrophotometry, adopting the analytical procedure described by Kurniawan *et al.* [18]. Spectral scanning was performed within the 200–400 nm range at a rate of 1,500 nm/minute, using a fixed bandwidth of 2.0 nm and data intervals of 1,000 nm. The maximum absorbance wavelength (λ_{max}) for the lapachol derivatives standard was identified at 330 nm (naphthoquinones) [19]. A 100 ppm stock solution was prepared by dissolving 5 mg of purified lapachol derivative in 50 ml of methanol. Calibration curves constructed through serial dilution (100–1.56 ppm) exhibited a strong linear response, with a correlation coefficient (R^2) of 0.9998.

2.5. Preparation of lapachol derivatives

Compounds (1), (2), and (3), isolated from the bark of *T. aurea*, were dissolved in dimethyl sulfoxide (DMSO) to prepare stock solutions at a concentration of 4 mg/ml. Aliquots of the prepared stocks were transferred to 96-well microplates (Falcon, USA), ensuring the final DMSO concentration in each well did not exceed 0.1% to maintain cell viability.

2.6. Cancer cell lines culture

The cytotoxic assay method used is based on the advanced of procedure by Kurniawan *et al.* [20]. The cytotoxic potential of lapachol derivative compounds isolated from the bark of *T. aurea* was evaluated against three human cancer cell lines: HeLa [human cervical epithelium, European Collection of Authenticated Cell Cultures (ECACC) 93021013], MCF-7

(breast adenocarcinoma, ECACC 86012803), and A549 (lung carcinoma, ECACC). All cell lines were cultured according to the standard protocol established by the ECACC. Cells were maintained in Dulbecco's Modified Eagle Medium (Dulbecco's Modified Eagle Medium (DMEM), Sigma-Aldrich), supplemented with 10% fetal bovine serum (Sigma-Aldrich) and 1× antimycotic solution (Sigma-Aldrich), in a humidified incubator set at 37°C with 5% CO₂. Once cell confluence reached approximately 80%–90%, the growth medium was aspirated, and cells were rinsed with phosphate-buffered saline (PBS, pH 7.4, Sigma-Aldrich). Detachment was performed using 0.05% Trypsin-ethylenediaminetetraacetic acid (Gibco, USA), followed by subculturing in fresh DMEM. Cell viability and confluency were determined using the trypan blue exclusion assay (0.4% Trypan Blue, Gibco, USA). For cytotoxicity testing, cells were seeded at a density of 1 × 10⁴ cells per well in 100 µl volumes into 96-well microplates and incubated overnight at 37°C under 5% CO₂ to allow adherence and recovery before treatment.

2.7. MTT-based cytotoxic assay

The cell viability was evaluated using the MTT assay (3-(4,5-dimethylthiazol-2-yl)-2,5-diphenyltetrazolium bromide), commonly referred to as the thiazole blue method. A range of compound concentrations was introduced to seeded cells in 96-well plates. Following a 48-hour incubation at 37°C under 5% CO₂, the media were aspirated, and wells were gently rinsed with (PBS, pH 7.4). Subsequently, 100 µl of MTT solution (5 mg/ml in PBS; Thermo Scientific) was added to each well (final concentration of 0.4–0.5 mg/ml), and plates were incubated for 4 hours to facilitate formazan production. After removal of the MTT solution, 100 µl of DMSO was added per well to solubilize the resulting formazan crystals. The absorbance was measured at 540 nm using a microplate enzyme-linked immunosorbent assay reader spectrophotometer. The measurements performed in triplicate, cell viability was expressed as a percentage relative to untreated control cells, calculated using the equation: % Viability cell = Abs of preserved cell (sample)/Abs of nonpreserved cell (control).

3. RESULTS AND DISCUSSION

In this study, three lapachol-derived compounds were successfully isolated with varying yields. Compound **(1)** was obtained as the foremost product, weighing 23.6 mg, followed by compound **(2)** (16.7 mg) and compound **(3)** (13.9 mg). The structural identification of each isolate was carried out by a comprehensive analysis of its spectroscopic data. The characteristic chemical shifts and coupling patterns observed in the ¹H and ¹³C NMR spectra of each compound showed high consistency with known data, supporting the accurate assignment of their structures. The Compound **(1)**: yellow needle-shaped crystals; mp 139.67 °C–141.11 °C [lit (21)]. 140°C–141°C; UV (MeOH) λ_{max} (log ε) 278 (2.47), 330 (1.27) nm; ¹H NMR data (CDCl₃, 500 MHz) δ 8.01 (2H, *dd*), 7.60 (2H, *d*), 3.25 (2H, *d*, *J* = 8.1 Hz), 5.11 (1H, *m*), 1.54 (3H, *s*), 1.73 (3H, *s*); ¹³C NMR (CDCl₃, 125 MHz) δ 181.8 (C-1), 153.8 (C-2), 123.7 (C-3), 185.1 (C-4), 126.7 (C-5), 134.8 (C-6), 132.7 (C-7), 126.5 (C-8), 129.4 (C-9), 133.7 (C-10),

22.55 (C-11), 119.6 (C-12), 133.7 (C-13), 25.6 (C-14), 17.9 (C-15); Molecular ion peak (EIMS) *m/z* 242 [M]⁺ (lit (19)). *m/z* 241 [M-H]⁺, *m/z* 225 [M-OH]⁺, *m/z* 157 [M-86]⁺. The Compound **(2)**: yellow formless crystal; mp 113.11°C–114.43°C [lit (21)]. 113°C–114°C; UV (MeOH) λ_{max} (log ε) 251 (3.34), 282 (2.22), 330 (2.13) nm; The ¹H NMR data (CDCl₃, 500 MHz) δ 8.11 (2H, *dd*), 7.66 (2H, *td*), 1.83 (2H, *t*, *J* = 6.6 Hz), 2.63 (2H, *t*, *J* = 6.6 Hz), 1.44 (6H, *s*); ¹³C NMR (CDCl₃, 125 MHz) δ 179.9 (C-1), 154.5 (C-2), 120.1 (C-3), 184.2 (C-4), 125.9 (C-5), 133.7 (C-6), 132.8 (C-7), 126.2 (C-8), 131.1 (C-9), 132.1 (C-10), 16.65 (C-11), 31.36 (C-12), 78.1 (C-13), 26.5 (2C-14/15). Molecular ion peak *m/z* 242 [M]⁺ [lit (19)]. *m/z* 243 [M+H]⁺, *m/z* 157 [M-86]⁺. The Compound **(3)**: orange crystalline; mp 153.68°C–154.29°C [lit (15)]. 154°C–156°C; UV (MeOH) λ_{max} (log ε) 256 (4.71), 282 (4.33), 330 (3.73) nm; The ¹H NMR data (CDCl₃, 500 MHz) δ 8.7 (1H, *dd*, *J* = 6.9), 7.62 (2H, *td*), 7.82 (1H, *dd*), 1.87 (2H, *t*), 2.58 (2H, *t*, *J* = 6.9), 1.46 (6H, *s*); ¹³C NMR (CDCl₃, 125 MHz) δ 179.7 (C-1), 178.4 (C-2), 112.6 (C-3), 161.9 (C-4), 123.9 (C-5), 133.7 (C-6), 130.5 (C-7), 128.3 (C-8), 129.8 (C-9), 132.5 (C-10), 16.00 (C-11), 31.5 (C-12), 79.2 (C-13), 26.6 (C-14), 26.7 (C-15). Molecular ion peak *m/z* 242 [M]⁺ (lit (19)). *m/z* 243 [M+H]⁺, *m/z* 226 [M-O]⁺, *m/z* 142 [M-101]⁺. The comparative evaluation against reference spectra from previously reported literature confirmed the identity of compound **(1)** as lapachol, compound **(2)** as α-lapachone, and compound **(3)** as β-lapachone [19,21,22]. The structure numbering of lapachol derivatives accustomed from the formal terms, based on the aliphatic side chain of lapachol and the pyran ring of both lapachones, to simplify structural comparison (Fig. 1).

Lapachol **(1)**, recognized by infrared (IR) spectral analysis, revealed a broad absorption band at 3,415 cm⁻¹, which is characteristic of the hydroxyl group, and a strong band at 1,667 cm⁻¹, assigned to the stretching vibrations of the conjugated C=O groups in the quinone moiety. Additional bands observed at 1,595 and 1,580 cm⁻¹ were attributed to aromatic C=C stretching modes, supporting the presence of a substituted naphthoquinone system [22]. The structure was further confirmed by ¹H NMR spectroscopy (500 MHz, CDCl₃), which revealed characteristic resonances: two singlets at δ 1.54 and 1.73 ppm, corresponding to methyl groups; a doublet at δ 3.25 ppm (2H, CH₂), a multiplet at δ 5.14 ppm (1H, olefinic CH), and aromatic protons appearing as multiplets at δ 7.60 ppm (2H) and δ 8.02 ppm (2H) [10,23]. The ¹H NMR spectrum showed characteristic singlets at δ 1.44 ppm (6H, CH₂), triplets at δ 1.83 and 2.63 ppm (4H, CH₂), and aromatic protons at δ 7.66 and 8.11 ppm (each 2H, multiplet), consistent with the

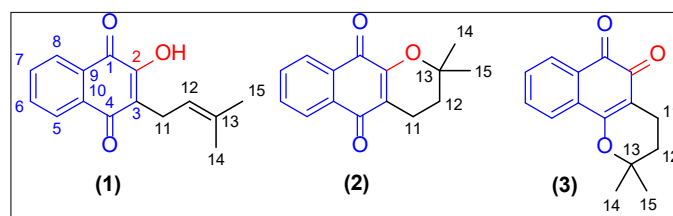


Figure 1. The Lapachol derivatives structure from *T. aurea*: compounds **(1)** lapachol, **(2)** α-lapachone, and **(3)** β-lapachone.

reported structure of α -lapachone (**2**) [10,24], identified by the IR spectrum displayed two prominent carbonyl stretching bands at 1,682 and 1,677 cm^{-1} , corresponding to C(1)=O modes in the quinone ring. A third strong absorption at 1,636 cm^{-1} was assigned to the C(4)=O group, while a medium-intensity band at 1,612 cm^{-1} was attributed to the C=C stretching mode within the quinonoid system [22]. The third compound was confirmed as β -lapachone (**3**), identified by ^1H NMR spectrum, which exhibited two methyl singlets at δ 1.46 ppm (6H), a methylene singlet at δ 1.87 ppm (2H), and a triplet at δ 2.58 ppm (2H, CH_2). The aromatic proton region displayed at δ 7.62 (2H), 7.82 (1H), and 8.70 ppm (1H), each corresponding to aromatic correlated protons. In the IR spectrum, three key absorptions were observed: a carbonyl stretch at 1,695 cm^{-1} for the C(1)=O group and a pair of closely spaced bands at 1,644 and 1,634 cm^{-1} , both corresponding to the C(2)=O stretching vibrations [22]. In addition, a strong band at 1,570 cm^{-1} was assigned to the quinonoid C=C stretching mode, differentiating β -lapachone from its isomers [23]. The combination of ^1H NMR and IR data confirms the structures and differentiates among lapachol, α -lapachone, and β -lapachone. The observed variations in IR carbonyl and C=C stretching regions (1,725–1,525 cm^{-1}) as well as aromatic proton shifts in NMR provide key evidence supporting the formation of the intramolecular pyran ring in both lapachone isomers [25]. Compound (**1**) exhibited a molecular ion at m/z 242 $[\text{M}]^+$ with characteristic fragments at m/z 225 $[\text{M}-\text{OH}]$ and m/z 157 $[\text{M}-86]$, indicating facile hydroxyl loss and prenyl side-chain cleavage. Compound (**2**) also showed m/z 242 $[\text{M}]^+$ with a protonated ion m/z 243 $[\text{M}+\text{H}]^+$ and a diagnostic fragment at m/z 157, consistent with scission of the substituted heterocyclic moiety. Compound (**3**) displayed m/z 242 $[\text{M}]^+$

and prominent ions m/z 226 $[\text{M}-\text{O}]$ and m/z 142 $[\text{M}-101]$, reflecting sequential oxygen loss and extensive quinonoid ring fragmentation.

The cytotoxic activities of lapachol derivatives, isolated from the bark of *T. aurea*, were evaluated against HeLa, MCF-7, and A549 cell lines, through doxorubicin used as a positive control (Table 1). Among the tested compounds, β -lapachone consistently exhibited the highest cytotoxicity across all cell lines (Fig. 2), with IC_{50} values of 6.24 ± 0.52 μM (HeLa), 5.61 ± 0.88 μM (A549), and 2.85 ± 0.26 μM (MCF-7).

These values approach those of doxorubicin, indicating strong antiproliferative potential. α -Lapachone displayed moderate activity, particularly against HeLa ($\text{IC}_{50} = 8.53 \pm 0.77$ μM) and MCF-7 ($\text{IC}_{50} = 13.57 \pm 1.26$ μM), but was less potent against A549 ($\text{IC}_{50} = 20.69 \pm 0.34$ μM). In contrast, lapachol showed the weakest cytotoxic effect, with IC_{50} values exceeding 10 μM in all tested cell lines, suggesting that cyclization to the pyran ring in lapachones substantially enhances cytotoxic activity [14,16,25].

Table 1. Cytotoxic activity of isolated lapachol derivatives from bark of *T. aurea*.

Compounds	IC_{50} (μM)		
	HeLa	MCF-7	A549
Lapachol	16.62 ± 2.18	27.22 ± 1.49	10.75 ± 1.71
α -lapachone	8.53 ± 0.77	13.57 ± 1.26	20.69 ± 0.34
β -lapachone	6.24 ± 0.52	2.85 ± 0.26	5.61 ± 0.88
Doxorubicin	2.93 ± 0.33	5.13 ± 0.81	3.35 ± 0.45

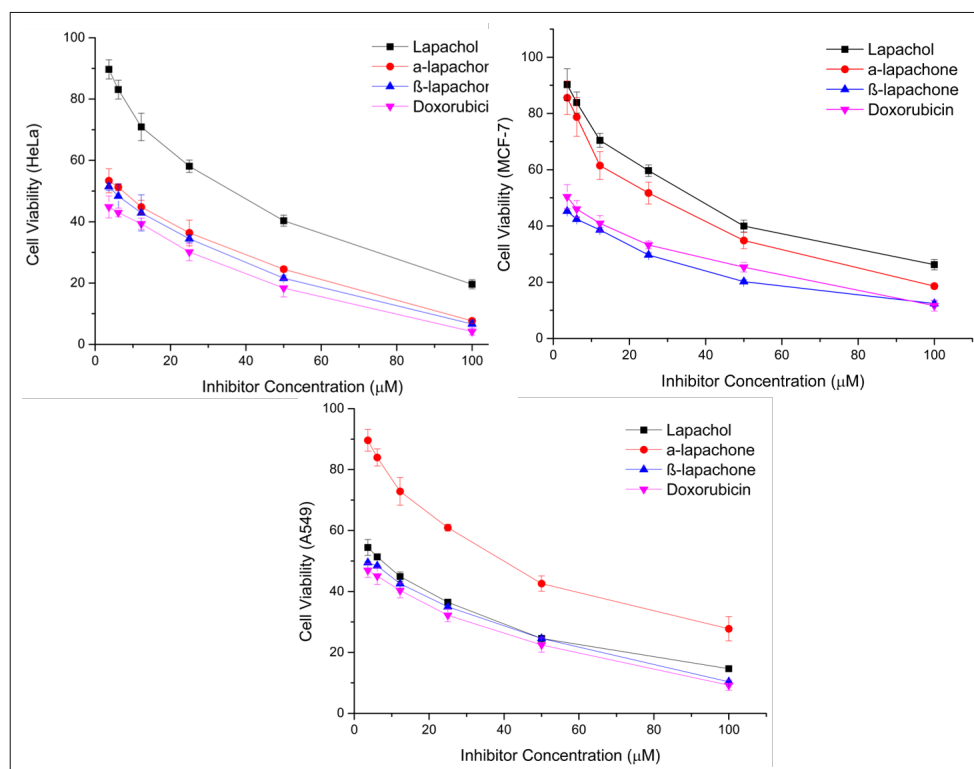


Figure 2. Cell viability chart of lapachol derivatives from the bark of *T. aurea*.

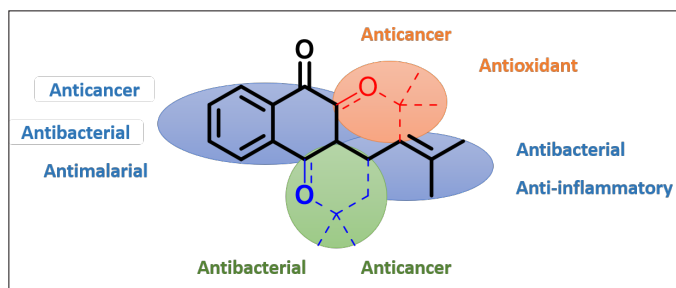


Figure 3. Chemical structure of lapachol derivatives and their literature therapeutic abilities [5,14,13,27]

The observed trend in activity (β -lapachone $>$ α -lapachone $>$ lapachol) is consistent with previous reports on quinone-containing natural products, where the presence and orientation of the fused pyran ring influence redox potential and deoxyribonucleic acid (DNA)-damaging capability (Fig. 3). These results highlight β -lapachone as a promising lead structure for further anticancer drug development, especially for lung carcinoma treatment [7]. Structure-activity relationship analysis suggests that chemical modification to preserve the β -lapachone scaffold while optimizing substituents could further enhance activity and selectivity [26]. The lapachol (1) evidently reduced rat brain microvascular endothelial cell viability and demonstrated superior activity against glioma C6 cells compared to temozolomide [14,23]. These results underscore the potential of lapachol and its analogs as promising scaffolds for anticancer drug development, warranting further mechanistic and *in vivo* evaluation [11,25]. The synthesized lapachol analog, obtained via a three-component reaction of 2-hydroxy-1,4-naphthoquinone, 2-phenylindole, and 4-nitrobenzaldehyde, exhibited notable cytotoxicity against breast (HeLa, IC_{50} 6.52 μ M) and liver hepatocellular (HepG2, IC_{50} 12.97 μ M) cancer cells [1,2,27]. Catalytic hydrogenation of lapachol derivatives yielded analogs with broad-spectrum anticancer activity against lung (NCI-460), renal (786-0), melanoma (UACC62), breast (MCF-7, NCI-ADR), ovarian (OVCAR03), and prostate (PC-03) cancer lines [16,28,27]. Lapachol (1) displayed moderate cytotoxicity against HeLa (IC_{50} = 19.04 \pm 0.7 μ g/ml); PC₃ (IC_{50} = 20.51 \pm 0.39 μ g/ml); 3T3 (IC_{50} = 6.15 \pm 0.55 μ g/ml) cells, indicating a structure-activity relationship favoring β -lapachone derivatives [11,15,29]. The β -Lapachone (2) exhibited potent and broad-spectrum anticancer activity across multiple cancer cell lines, with IC_{50} values in the low micromolar range. Notably, it showed remarkable cytotoxicity toward breast (MCF-7; IC_{50} = 1.45 μ M), colon (HT-29; IC_{50} = 1.99 μ M), prostate (Du-145; IC_{50} = 1.10 μ M), ovarian (SK-OV3; IC_{50} = 1.18 μ M), pancreatic (PaCa-3; IC_{50} = 1.52 μ M), and lung (A549; IC_{50} = 1.79 μ M) cancer cells, while sparing normal cells [12,14,27]. *In vivo*, treatment reduced tumor volume by up to 75% without observable toxicity. Mechanistically, β -lapachone induced G₁/S phase arrest, apoptosis, and necrosis via cytochrome C release and caspase-3 activation. Structure-activity analysis revealed that C-3 hydroxyl substitution reduced activity toward HT-29 and A549 cells but enhanced activity against BE colon cancer cells [16,24,10]. These findings underscore β -lapachone's potential

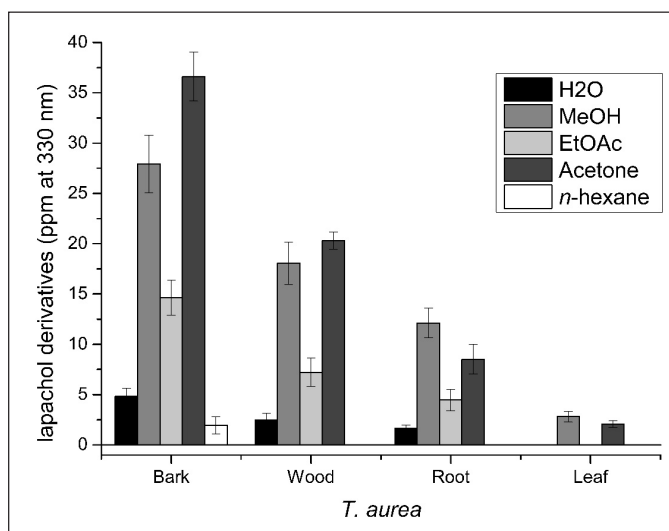


Figure 4. Lapachol derivatives content of *T. aurea*.

Table 2. The lapachol derivatives (naphthoquinones) are found in numerous parts of *T. aurea*.

<i>Tabebuia aurea</i>	Lapachol derivatives (ppm)				
	H ₂ O	MeOH	EtOAc	Acetone	n-hexane
Bark	4.82 ± 0.79	27.93 ± 2.86	14.64 ± 1.72	36.62 ± 2.44	1.96 ± 0.84
Wood	2.47 ± 0.66	18.05 ± 2.11	7.22 ± 1.39	20.31 ± 0.84	n.d.
Root	1.63 ± 0.35	12.11 ± 1.49	4.47 ± 1.07	6.50 ± 1.47	n.d.
Leaf	n.d.	2.82 ± 0.52	n.d.	2.07 ± 0.35	n.d.

*n.d not detected.

as a selective anticancer agent with distinct cell cycle effects compared to conventional DNA-damaging agents [11,14]. Early preclinical studies reported notable antiproliferative effects, which prompted its advancement into Phase I clinical trials. However, these trials revealed substantial systemic toxicity and insufficient therapeutic efficacy at tolerable concentration levels. Consequently, the National Cancer Institute discontinued the clinical development of lapachol.

The α -Lapachone (2) analogs exhibited antiangiogenic activity *in vivo*, reducing tumor vascular volume and length without affecting vessel diameter. Treatment markedly prolonged tumor volume doubling time in E0771 and 4T1 models, with no associated weight loss, indicating favorable safety [21,13]. Mice tolerated intraperitoneal doses up to 100 mg/kg without toxicity. *In vitro*, the analogs showed moderate cytotoxicity toward breast, glioma (SF268), lung (NCI-H460), and HepG2 cancer cells, supporting their potential as safe antitumor agents [11,27]. β -Lapachone (2) exhibited the highest cytotoxicity against WHCO1 cells (IC_{50} = 1.6 μ M), surpassing cisplatin by ~10 fold. 3-Bromo- β -lapachone and nor- β -lapachone showed comparable activity (IC_{50} = 1.8 and 2.4 μ M, respectively). In contrast, 2-deoxylapachol, lapachol, and α -lapachone were less active (IC_{50} = 15.0–28.7 μ M) [14,11].

The content analysis of lapachol derivatives from numerous parts of *T. aurea* revealed distinct variations in metabolite distribution and solvent affinity (Fig. 4). The bark exhibited the highest overall content across most solvents, with acetone extracts yielding the greatest concentration, followed by methanol and ethyl acetate by 36.62 ± 2.44 , 27.93 ± 2.86 , and 14.64 ± 1.72 ppm, respectively (Table 2). The bark of *T. aurea* is the main reservoir of lapachol derivatives, describing bark tissues as major storage sites for naphthoquinones [1,26]. In comparison, wood samples demonstrated moderate accumulation, with acetone (20.31 ± 0.84 ppm) and methanol (18.05 ± 2.11 ppm) extracts showing appreciable yields. Root extracts displayed considerably lower levels, with maximum detection in methanol (12.11 ± 1.49 ppm), suggesting that lapachol derivatives allocation is less pronounced in underground tissues [25,27]. The leaf exhibited the lowest detectable concentrations, with only trace levels observed in methanol (2.82 ± 0.52 ppm) and acetone (2.07 ± 0.35 ppm), while no derivatives were detected in other solvents.

Solvent polarity strongly influenced extraction efficiency. Acetone and methanol consistently yielded higher contents across all tissues, underscoring their effectiveness in recovering moderately polar to polar lapachol derivatives. In contrast, *n*-hexane extracts were negligible or undetectable in most tissues, reflecting the poor solubility of these compounds in nonpolar media [7]. These findings are important as they demonstrate that both plant part selection and solvent polarity critically affect the recovery of lapachol derivatives [3]. The high concentration in bark-acetone extracts suggests this matrix-solvent combination as the most suitable source for bioactive naphthoquinones from *T. aurea* [3]. Such insights are essential for guiding pharmacognostic investigations and optimizing extraction strategies for therapeutic applications. These findings highlight the importance of informed and responsible utilization, and they suggest that widespread or excessive use of *Tabebuia* in traditional medicine should be approached carefully until safety profiles are more comprehensively established.

4. CONCLUSION

This study demonstrates the phytochemical diversity of *T. aurea* (Bignoniaceae), a species traditionally associated with medicinal use, through systematic phytochemical screening and spectroscopic analysis. Three lapachol-derived naphthoquinones-lapachol (**1**), α -lapachone (**2**), and β -lapachone (**3**), were successfully isolated and structurally characterized from the bark of *T. aurea*. Among the tested extracts, the acetone bark extract yielded the highest concentration of naphthoquinone derivatives (36.62 ± 2.44 ppm), underscoring the influence of solvent polarity and plant tissue on metabolite recovery. β -Lapachone exhibited the strongest antiproliferative activity against HeLa, MCF-7, and A549 cancer cell lines, with IC_{50} values ranging from 2.85 to 6.24 μ M, approaching the activity of doxorubicin under the same *in vitro* conditions. These findings indicate that lapachol derivatives from *T. aurea* possess promising bioactivity at the cellular level; however, their pharmacological relevance should be interpreted cautiously in the absence of *in vivo* or clinical validation. While the results provide a chemical and biological basis that may be relevant

to the traditional use of *T. aurea*, further ethnopharmacological and *in vivo* studies are required to substantiate such claims. Future research should focus on mechanistic studies, toxicity evaluation, and biological validation to better define the therapeutic potential of lapachol-based compounds derived from this species.

5. ACKNOWLEDGMENTS

The authors gratefully acknowledge the support from LPPM of Institut Teknologi Sumatera (ITERA) for research funding (Grant No. 1539b/IT9.2.1/PT.01.03/2024). We also thank the ITERA Botanical Garden for providing the plant samples.

6. AUTHOR CONTRIBUTIONS

All authors made substantial contributions to conception and design, acquisition of data, or analysis and interpretation of data; took part in drafting the article or revising it critically for important intellectual content; agreed to submit to the current journal; gave final approval of the version to be published; and agree to be accountable for all aspects of the work. All the authors are eligible to be author as per the International Committee of Medical Journal Editors (ICMJE) requirements/guidelines.

7. CONFLICT OF INTEREST

The authors report no financial or any other conflicts of interest in this work.

8. ETHICAL APPROVALS

This study does not involve experiments on animals or human subjects.

9. DATA AVAILABILITY

All data generated and analyzed are included in this research article.

10. PUBLISHER'S NOTE

All claims expressed in this article are solely those of the authors and do not necessarily represent those of the publisher, the editors and the reviewers. This journal remains neutral with regard to jurisdictional claims in published institutional affiliation.

11. USE OF ARTIFICIAL INTELLIGENCE (AI)-ASSISTED TECHNOLOGY

The authors declare that they have not used artificial intelligence (AI)-tools for writing and editing of the manuscript, and no images were manipulated using AI.

REFERENCES

- Gómez Castellanos JR, Prieto JM, Heinrich M. Red Lapacho (*Tabebuia impetiginosa*)-A global ethnopharmacological commodity. *J Ethnopharmacol.* 2009;121(1):1-3. doi: <https://doi.org/10.1016/j.jep.2008.10.004>
- Ryan RYM, Fernandez A, Wong Y, Miles JJ, Cock IE. The medicinal plant *Tabebuia impetiginosa* potentially reduces pro-inflammatory cytokine responses in primary human lymphocytes. *Scientific Rep.* 2021;11:5519. doi: <https://doi.org/10.1038/s41598-021-85211-8>

3. Hamed ANE, Mahmoud BK, Samy MN, Kamel MS. An extensive review on genus "*Tabebuia*", family bignoniaceae: phytochemistry and biological activities (1967 to 2018) [Internet]. *J Herbal Med.* 2020;24:100410. doi: <https://doi.org/10.1016/j.hermed.2020.100410>
4. Chandra S, Gahlot M, Choudhary AN, Palai S, De Almeida RS, De Vasconcelos JEL, *et al.* Scientific evidences of anticancer potential of medicinal plants [Internet]. *Food Chem Adv.* 2023;2:100239. doi: <https://doi.org/10.1016/j.focha.2023.100239>
5. Angulo -Elizari E, Henriquez-Figueroa A, Morán-Serradilla C, Plano D, Sanmartín C. Unlocking the potential of 1,4-naphthoquinones: a comprehensive review of their anticancer properties. *Eur J Med Chem.* 2024;268(3):116249. doi: <https://doi.org/10.1016/j.ejmech.2024.116249>
6. Franco K, Gonçalves G, Naomi N, Cristina M, Alexandre C, Brentan D, *et al.* *Tabebuia aurea* decreases hyperalgesia and neuronal injury induced by snake venom. 2019;233(August 2018):131–40.
7. El-Hawary SS, Taher MA, Amin E, AbouZid SF, Mohammed R. Genus *Tabebuia*: a comprehensive review journey from past achievements to future perspectives. *Arab J Chem* [Internet]. 2021;14(4):103046. Available from: <https://doi.org/10.1016/j.arabjc.2021.103046>
8. Nahar J, Morshed MN, Rupa EJ, Lee JH, Kariyath Valappil A, Awais M, *et al.* Roasting Extract of *Handroanthus impetiginosus* Enhances Its Anticancer Activity in A549 Lung Cancer Cells and Improves Its Antioxidant and Anti-Inflammatory Effects in Normal Cells. *Appl Sci.* 2023;13(24):13171. doi: <https://doi.org/10.3390/app132413171>
9. Quadros Gomes AR, Da Rocha Galucio NC, De Albuquerque KCO, Brígido HPC, Varela ELP, Castro ALG, *et al.* Toxicity evaluation of *Eleutherine plicata* Herb. extracts and possible cell death mechanism. *Toxicol Rep.* 2021;8:1480–7. doi: <https://doi.org/10.1016/j.toxrep.2021.07.015>
10. Ríos-Luci C, Bonifazi EL, León LG, Montero JC, Burton G, Pandiella A, *et al.* B-Lapachone analogs with enhanced antiproliferative activity [Internet]. *Eur J Med Chem Internet.* 2012;53:264–74. doi: <https://doi.org/10.1016/j.ejmech.2012.04.008>
11. Hussain H, Green IR. Lapachol and lapachone analogs: a journey of two decades of patent research(1997-2016) [Internet]. *Expert Opin Ther Pat Internet.* 2017;27(10):1111–21. doi: <https://doi.org/10.1080/13543776.2017.1339792>
12. Ventura Pinto A, Lisboa De Castro S. The trypanocidal activity of naphthoquinones: a review. *Molecules.* 2009;14(11):4570–90. doi: <https://doi.org/10.3390/molecules14114570>
13. Peixoto JF, Oliveira A da S, Gonçalves - Oliveira LF, Souza - Silva F, Alves CR. Epoxy- α -lapachone (2,2-Dimethyl-3,4-dihydro-spiro[2H-naphtho2,3-bpyran-10,2'-oxirane-5(10H)-one]): a promising molecule to control infections caused by protozoan parasites. *Braz J Infect Dis.* 2023;27(2):102743. doi: <https://doi.org/10.1016/j.bjid.2023.102743>
14. Gong Q, Hu J, Wang P, Li X, Zhang X. A comprehensive review on β -lapachone: mechanisms, structural modifications, and therapeutic potentials [Internet]. *Eur J Med Chem Internet.* 2021;210:112962. doi: <https://doi.org/10.1016/j.ejmech.2020.112962>
15. Gomes CL, De Albuquerque Wanderley Sales V, Gomes De Melo C, Ferreira Da Silva RM, Vicente Nishimura RH, Rolim LA, *et al.* Beta-lapachone: natural occurrence, physicochemical properties, biological activities, toxicity and synthesis. *Phytochemistry.* 2021;186:112713. doi: <https://doi.org/10.1016/j.phytochem.2021.112713>
16. Sunassee SN, Veale CGL, Shunmoogam-Gounden N, Osoniyi O, Hendricks DT, Cairra MR, *et al.* Cytotoxicity of lapachol, β -lapachone and related synthetic 1,4-naphthoquinones against oesophageal cancer cells [Internet]. *Eur J Med Chem Internet.* 2013;62(2013):98–110. doi: <https://doi.org/10.1016/j.ejmech.2012.12.048>
17. Kurniawan R, Azis S, Maulana S, Ashari A, Prasetyo BA, Suhartati T, *et al.* The cytotoxicity studies of phytosterol discovered from *Rhizophora apiculata* against three human cancer cell lines. *J Appl Pharm Sci.* 2023;13(1):156–62. doi: <https://doi.org/10.7324/JAPS.2023.130115>
18. Kurniawan R, Sukrasno S, Ashari A, Suhartati T. Diving into paclitaxel: isolation and screening content from *Taxus sumatrana* at Singgalang Conservation Center, West Sumatra [Internet]. *Nat Prod Res Internet.* 2024;0(0):1–5. doi: <https://doi.org/10.1080/14786419.2024.2312540>
19. Bai L, Han Y, Yao J, Li X, Li Y, Xu P, *et al.* Structural elucidation of the metabolites of lapachol in rats by liquid chromatography-tandem mass spectrometry [Internet]. *J Chromatogr B Anal Technol Biomed Life Sci.* 2014;944:128–35. doi: <https://doi.org/10.1016/j.jchromb.2013.11.024>
20. Kurniawan R, Saleh M, Arif Ashari, Hawa Purnama, Muhammad Yogi Saputra, Tati Suhartati, *et al.* The Evaluation of α -amyrin from *Callistemon Citrinus*: A Study on Distribution and Cytotoxic Properties. *Trends in Sciences.* 2025;28;22(4):9436–6. doi: <https://doi.org/10.48048/tis.2025.9436>
21. Edet A, Olorunfemi E, Aniebi E, Isiguzoro I. Changes in serum zinc, magnesium and copper in sickle cell patients: a case study in Jos, Nigeria. *Afr J Pharm Pharmacol.* 2015;9(1):53–9. doi: <https://api.semanticscholar.org/CorpusID:212526486>
22. Delarmelina M, Ferreira GB, Ferreira VF, De M. Carneiro JW. Vibrational spectroscopy of lapachol, α - and β -lapachone: theoretical and experimental elucidation of the Raman and infrared spectra [Internet]. *Vib Spectrosc.* 2016;86:311–23. doi: <https://doi.org/10.1016/j.vibspec.2016.08.009>
23. Salas C, Tapia RA, Ciudad K, Armstrong V, Orellana M, Kemmerling U, *et al.* *Trypanosoma cruzi*: activities of lapachol and α - and β -lapachone derivatives against epimastigote and trypomastigote forms. *Bioorganic Med Chem.* 2008;16(2):668–74. doi: <https://doi.org/10.1016/j.bmc.2007.10.038>
24. Du L, Li MD, Zhang Y, Xue J, Zhang X, Zhu R, *et al.* Photoconversion of β -Lapachone to α -Lapachone via a Protonation-Assisted Singlet Excited State Pathway in Aqueous Solution: a Time-Resolved Spectroscopic Study. *J Org Chem.* 2015;80(15):7340–450. doi: <https://doi.org/10.1021/acs.joc.5b00086>
25. Ravelo AG, Estevez-Braun A, Perez-Sacau E. The Chemistry and Biology of Lapachol and Related Natural Products: α - and β -Lapachones. *ChemInform.* 2004;35(31):719–59. doi: [https://doi.org/10.1016/S1572-5995\(03\)80017-0](https://doi.org/10.1016/S1572-5995(03)80017-0)
26. Arbain D, Sriwahyuni K, Susanti D, Taher M. Genus *Eleutherine*: a review of its distribution, traditional uses, phytochemistry, biological activities and their interchange names [Internet]. *South Afr J Bot Internet.* 2022;150:731–43. doi: <https://doi.org/10.1016/j.sajb.2022.08.022>
27. Atolani O, Olatunji GA, Adeyemi OS. Cytotoxicity of Lapachol and Derivatized Analogues from *Kigelia africana* (Lam.) Benth. on Cancer Cell Lines [Internet]. *Arab J Sci Eng Internet.* 2021;46(6):5307–12. doi: <https://doi.org/10.1007/s13369-020-05113-1>
28. Kumari P, Singh V, Kant V, Ahuja M. Current status of 1,4-Naphthoquinones and their derivatives for wound healing. *Eur J Med Chem Rep.* 2024;12:100194. doi: <https://doi.org/10.1016/j.ejmcr.2024.100194>
29. Khan J, Rani A, Aslam M, Pandey G, Nand Pant B. A review on the synthesis and application of naphthoquinone-based drugs [Internet]. *Results Chem Internet.* 2023;6:101138. doi: <https://doi.org/10.1016/j.rechem.2023.101138>

How to cite this article:

Kurniawan R, Ashari A, Saputra MY, Indarto I, Ahmadi P, Suhartati T. The lapachol derivatives from *Tabebuia aurea*: distribution and cytotoxic evaluation against human cancer cells. *J Appl Pharm Sci.* 2026;16(05):162-168. DOI: 10.7324/JAPS.2026.285870